analytical chemistry

Article

pubs.acs.org/ac

Graphene Fluorescence Switch-Based Cooperative Amplification: A Sensitive and Accurate Method to Detection MicroRNA

Haiyun Liu,[†] Lu Li,[†] Qian Wang, Lili Duan, and Bo Tang*

College of Chemistry, Chemical Engineering and Materials Science, Collaborative Innovation Center of Functionalized Probes for Chemical Imaging, Key Laboratory of Molecular and Nano Probes, Ministry of Education, Shandong Normal University, Jinan, 250014 Shandong, People's Republic of China

Supporting Information

ABSTRACT: MicroRNAs (miRNAs) play significant roles in a diverse range of biological progress and have been regarded as biomarkers and therapeutic targets in cancer treatment. Sensitive and accurate detection of miRNAs is crucial for better understanding their roles in cancer cells and further validating their function in clinical diagnosis. Here, we developed a stable, sensitive, and specific miRNAs detection method on the basis of cooperative amplification combining with the graphene oxide (GO) fluorescence switch-based circular exponential amplification and the multimolecules labeling of SYBR Green I (SG). First, the target miRNA is adsorbed on the surface of GO, which can protect the miRNA from enzyme digest. Next, the miRNA hybridizes with a partial hairpin probe and then acts as a primer to initiate a strand displacement reaction to form a complete duplex. Finally, under the action of nicking enzyme, universal DNA fragments are released and used as triggers to initiate next reaction cycle, constituting a new circular exponential amplification. In the proposed strategy, a small amount of target miRNA can be converted to a large number of stable DNA triggers, leading to a remarkable amplification for the target. Moreover, compared with labeling with a 1:1 stoichiometric ratio, multimolecules binding of intercalating dye SG to double-stranded DNA (dsDNA) can induce significant enhancement of fluorescence signal and further improve the detection sensitivity. The extraordinary fluorescence quenching of GO used here guarantees the high signal-to-noise ratio. Due to the protection for target miRNA by GO, the cooperative amplification, and low fluorescence background, sensitive and accurate detection of miRNAs has been achieved. The strategy proposed here will offer a new approach for reliable quantification of miRNAs in medical research and early clinical diagnostics.

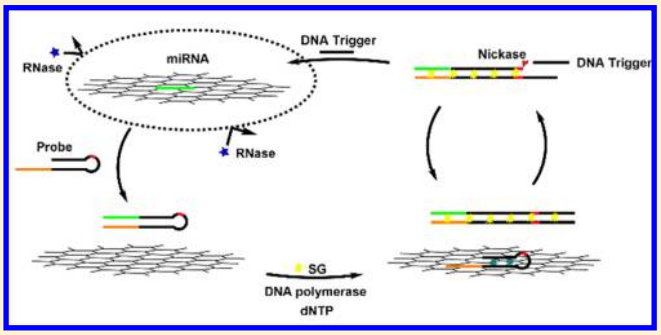

MicroRNAs (miRNAs) are a group of endogenous noncoding RNAs of about 18−24 nucleotides that can regulate the expression of target genes and play significant roles in a diverse range of biological progress such as cell proliferation, migration, and apoptosis.[1−5] Recent studies have found that some miRNAs exhibit altered expression in cancer cells.[6] Aberrant expression of miRNAs is associated with cancer initiation, tumor stage, and tumor response to treatments.[1,2] Now, miRNAs have been regarded as biomarkers and therapeutic targets in cancer treatment.[2,5−10] Therefore, effective detection of miRNAs is crucial for better understanding their roles in cancer cells and further validating their function in clinical diagnosis. Currently, the real-time polymerase chain reaction,[11] Northern blot,[12,13] and microarray technology have been widely used for miRNAs analysis.[14−19] Except these methods, various new strategies have been developed to improve the detection sensitivity and adaptability, such as nanomaterial-based assay,[20−24] bioluminescence-based assay,[25] modified invader assay,[26] ribozyme-based assay,[27] sequencing-based assay,[28] exponential amplification reaction (EXPAR) assay,[29] rolling circle amplification,[30] strand displacement assay,[31] and hairpin-based amplification.[32] Among these methods, the enzyme-based cyclic amplification has become increasingly popular in the miRNAs detection due to its simplicity, specificity, and high sensitivity.[33,34] However, in most reported enzyme-based cyclic amplification strategies, after the action of enzyme, the target miRNA was released and used as triggers to initiate next reaction cycle. The vulnerability of miRNA to enzymatic digestion will affect the accuracy and sensitivity of detection. So, new, sensitive, and accurate amplification strategies for miRNA analysis are critical and in urgent need.

Recently, graphene oxide (GO), a water-soluble and two-dimensional (2D) nanomaterial, has become extremely popular in biological applications due to its unique and excellent electronic, thermal, and mechanical properties.[35,36] It has been reported that single-stranded DNA (ssDNA) could interact strongly with GO and readily adsorb onto GO due to noncovalent $\pi-\pi$ stacking interactions between the hexagonal

Received: February 25, 2014
Accepted: May 12, 2014
Published: May 12, 2014

   dx.doi.org/10.1021/ac500752t | Anal. Chem. 2014, 86, 5487−5493

cells of graphene and the ring structure of nucleobases.[37] Specifically, through theoretical calculations, graphene has been predicted to be a superquencher with the long-range nanoscale energy transfer property.[38,39] Experiments also showed that GO can quench the fluorescence of dyes and dye-labeled ssDNA probes.[40,41] The extraordinary fluorescence quenching property of GO, in combination with the unique ssDNA/GO interactions, has been employed to elaborately design miRNAs sensors in homogeneous solution.[33,34,42,43] Moreover, researchers have proven that after noncovalent adsorption on GO surface, ssDNA and single-stranded RNA (ssRNA) probes were effectively protected from enzymatic digestion by nuclease due to a steric hindrance effect of GO that prevents nuclease from binding to the DNA and RNA,[41,44] which inspired us to constitute new graphene-based analysis platform for miRNAs.

Here, we developed a highly sensitive and accurate detection method of miRNAs on the basis of a GO fluorescence switch-based circular exponential amplification coupled with the multimolecules labeling of intercalating dye SYBR Green I (SG). First, the target miRNA can be protected from enzymatic digestion effectively after noncovalent adsorption on GO surface. Then the miRNA hybridizes with a designed partial hairpin probe and extends along the template to form a complete duplex. After that, the nicking endonuclease cleaves the sequences of duplex, producing a short DNA product to initiate the next reaction cycle. Finally, a new circular exponential amplification for the target miRNA can be achieved. In the proposed strategy, a small amount of miRNA can be converted to a large number of stable DNA triggers, leading to a remarkable amplification for the target. Unlike the miRNA that was released and used as triggers in most reported cyclic enzymatic amplification,[33,34] the released DNA triggers are more stable and preferred for the sustained reaction. Moreover, an intercalating dye SG is used for fluorescence detection. Compared with single dye labeling in usually used probes, multimolecules binding of SG to double-stranded DNA (dsDNA) can induce further amplification of fluorescence signal.[45] The GO, as a fluorescence switch, exhibits extraordinary fluorescence quenching, guaranteeing the high signal-to-noise ratio. Due to the protection for target miRNA by GO, the cooperative amplification, and the low fluorescence background, the new graphene fluorescence switch-based circular exponential amplification allows sensitive and accurate quantification of miRNA with a sensitivity of 10.8 fM. MiRNA analysis in human lung cells was also performed, indicating that this strategy will become a reliable and sensitive miRNAs quantification method in medical research and early clinical diagnostics.

EXPERIMENTAL SECTION

Materials and Apparatus. The HPLC-purified partial hairpin probes and microRNAs were purchased from TaKaRa Biotechnology Co., Ltd. (Dalian, China). The sequences of the partial hairpin probes and microRNAs are listed in Table 1. The diethyprocarbonated (DEPC)-treated deionized water, deoxynucleotides (dNTPs), TE buffer, cryonase, and ribonuclease inhibitor were obtained from TaKaRa Biotechnology Co., Ltd. (Dalian, China). The vent (exo-) DNA polymerase and nicking endonuclease Nt.BstNBI were purchased from New England Biolabs (Ipswich, Massachusetts). Graphene oxide was purchased from XF Nano, Inc. (Nanjing, China). SYBR Green I was purchased from Xiamen Zeesan Biotechnology Co., Ltd. (Xiamen, China). Fetal bovine serum was purchased from Gibco (Carlsbad, California). RPMI 1640 and MirVana miRNA isolation kit were purchased from Life Technologies (Carlsbad, California). DEPC-treated deionized water was used in all experiments.

Table 1. Sequences of Hairpin Probes and MicroRNAs[a]

name	sequence (5′−3′)
partial hairpin probe	5′-*ACT ATA CAA CCT ACT ACC* TTT CA**G ACT C**AC *GTA GTA GGT TGT ATA GTG* AAC TAT ACA ACC TAC TAC CTC AA-3′
complete hairpin probe	5′-*TTG AGG TAG TAG GTT GTA TAG TTC ACT ATA CAA CCT ACT ACC* TTT CA**G ACT C**AC *GTA GTA GGT TGT ATA GTG AAC TAT ACA ACC TAC TAC CTC AA*-3′
let-7a	5′-UGA GGU AGU AGG UUG UAU AGU U-3′
let-7b	5′-UGA GGU AGU AGG UUG U<u>G</u>U <u>G</u>GU U-3′
let-7c	5′-UGA GGU AGU AGG UUG UAU <u>G</u>GU U-3′
miR-21	5′-UAG CUU AUC AGA CUG AUG UUG A-3′
ssDNA−let-7a	5′-TGA GGT AGT AGG TTG TAT AGT T-3′
dsDNA−let-7a	5′-TGA GGT AGT AGG TTG TAT AGT T-3′
	3′-ACT CCA TCA TCC AAC ATA TCA A-5′

[a]The italicized region of the hairpin probe indicates the stem sequence, and bold characters indicate recognition sequences of Nt.BstNBI; the underlined bases are the different bases between let-7b, let-7c, and let-7a.

The amplification reaction was performed on a Veriti 96 well thermal cycler (Applied Biosystems, California). Gel electrophoresis was conducted using DYCZ-24DN electrophoresis cell (LIUYI, Beijing, China) and GelDoc-It imaging systems (UVP, Cambridge, U.K.). The fluorescent spectra were measured using Cary Eclipse fluorescence spectrophotometer (Varian, California).

Amplification Reaction. The amplification reaction was carried out with 44 μL of reaction mixture containing 1.25 μg of GO, 12 nM hairpin probe, 0.2 mM dNTPs, 1.5 U of vent (exo-) DNA polymerase, 12 U of Nt.BstNBI, 1.2 U of RNase inhibitor, 1× ThermoPol buffer [10 mM KCl, 10 mM $(NH_4)_2SO_4$, 20 mM Tris−HCl (pH 8.8), 2 mM $MgSO_4$, 0.1% Triton X-100], 1× Nt.BstNBI buffer [100 mM NaCl, 50 mM Tris−HCl (pH 8.8), 10 mM $MgCl_2$, 1 mM DTT], and different concentrations of target miRNA. Before the reaction, the partial hairpin probe was incubated at 95 °C for 5 min and then slowly cooled to room temperature over 30 min to make the probe perfectly fold into a hairpin structure. After annealing, the hairpin probes were added to the mixture and incubated at 55 °C for 2 h. The amplification product was then incubated with 6 μL of 20× SG for 10 min.

Digestion of miRNAs by Cryonase. MiRNA let-7a (10 μM) was mixed with 20 U of cryonase in the absence and presence of GO (25 μg/mL), respectively. Then the mixture was incubated at 37 °C for 0, 2, 5, 10, 30, 60, and 120 min, respectively. Afterward, the samples were heated to 95 °C for 15 min to deactivate cryonase and analyzed by 20% polyacrylamide gel electrophoresis (PAGE).

Measurement of Fluorescent Spectra. The fluorescent spectra were measured using a Cary Eclipse fluorescence spectrophotometer. The excitation wavelength was 494 nm, and the spectra were recorded between 500 and 650 nm. The fluorescence emission maximum was at 521 nm.

Gel Electrophoresis Analysis. The products of circular exponential amplification were analyzed by 16% PAGE. The products of digestion by cryonase were analyzed by 20% PAGE. The gel was carried in 1× electrophoresis Tris−borate−EDTA (TBE) buffer at 100 V for 2 h and stained with SG for 15 min.

dx.doi.org/10.1021/ac500752t | Anal. Chem. 2014, 86, 5487−5493

The imaging of the gel was performed using UVP GelDoc-It imaging systems.

Cell Lysis and RNA Preparation. The human lung cells (A549) were cultured according to instructions of the American Type Culture Collection. Cells were grown in RPMI 1640 (Hyclone, penicillin 100 U/mL, streptomycin 100 μg/mL) plus 10% fetal bovine serum (FBS, Gibco) and maintained at 37 °C in a humidified atmosphere of 5% CO_2 and 95% air. The cells were collected and centrifuged at 3000 rpm for 5 min in a culture medium, washed once with PBS buffer, and then spun down at 3000 rpm for 5 min. The cell pellets were suspended in 1 mL of lysis solution. Total RNA was extracted from human lung cells using the MirVana miRNA isolation kit according to the manufacturer's procedures. The sample of let-7a in these cells was diluted with RNase-free TE buffer (10 mM Tris−HCl, 1 mM EDTA, pH 7.5), then analyzed with the proposed miRNAs assays.

RESULTS AND DISCUSSION

Stability of GO-Protected Target miRNAs. One of the major challenges for the detection of miRNAs is their vulnerability to enzymatic digestion. Here, the protection effect of GO on miRNAs against enzymatic cleavage was investigated by gel electrophoresis experiments using let-7a as a target. Cryonase, a nonspecific endonuclease that can digest all types of DNA and RNA substrates, was chosen to digest the miRNA. As shown in Figure 1, at normal conditions without the protection of GO, let-7a was partially digested after incubation with cryonase for 2 min. After 5 min, the miRNA band became invisible, indicating complete enzymatic hydrolysis of the let-7a by cryonase. However, there was no obvious hydrolysis of the let-7a in the presence of GO even after 2 h. These results demonstrate that miRNA was protected from cryonase digestion after adsorption on the GO. As the references reported, the protection of miRNA by GO may be due to several reasons. Steric hindrance effect can prevent nuclease from binding to the miRNA. Conformational change of the miRNA may lead it to be unrecognizable for nuclease binding pockets. Changes in local ion concentration induced by GO may also be another factor.[40] So, the introduction of GO into the miRNA detection system will make the target more stable and further improve the accuracy and sensitivity of detection.

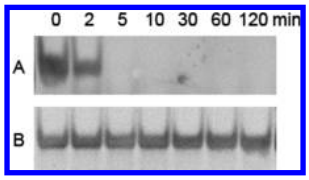

Figure 1. Gel electrophoresis analysis of target miRNA treated with cryonase in the absence (A) and presence (B) of GO.

Adsorption Selectivity of GO for Different Types of Nucleic Acids. It has been reported that GO can interact strongly with ssDNA and quench the fluorescence of dyes labeled on the ssDNA, while it has less affinity toward dsDNA.[37,46] On the basis of this finding, GO has been used as an effective platform for the biosensor.[47,48] In the proposed strategy, different forms of DNA such as ssDNA trigger, partial hairpin probe, and complementary dsDNA existed in the detection system. On one hand, in order to protect the miRNAs from enzymatic digestion and quench the fluorescence from the partial hairpin probe, GO is expected to interact with the single-strand miRNAs, ssDNA trigger, and the partial hairpin probe. On the other hand, GO is expected to be free from the complementary dsDNA and have no effect on the fluorescence from the dsDNA. So, the adsorption selectivity of different nucleic acids on GO surface was researched through the fluorescence detection. The results are shown in Figure 2.

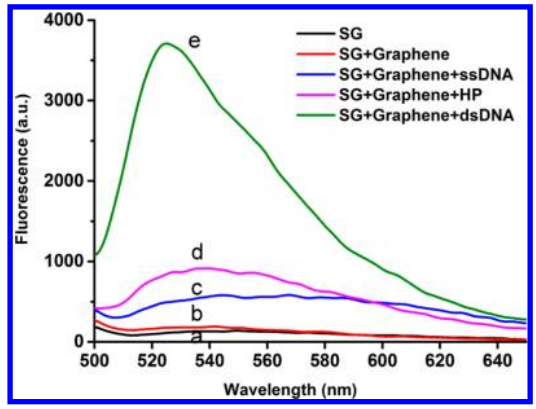

Figure 2. Fluorescence response of SG with different types of DNA in the presence of GO.

SG showed negligible autofluorescence (Figure 2, line a) and there was no apparent enhancement of the fluorescence of SG both in the presence of GO, GO and ssDNA (Figure 2, lines b and c). After the addition of SG into the system containing GO and partial hairpin probe, a slight fluorescence intensity could be detected (Figure 2, line d), which can be explained that the fluorescence of SG inserted into the double-strand fragment could be quenched mostly by GO as a result of reaction between the single-strand fragment of the partial hairpin probe and the GO.[38,39] Upon the addition of SG to dsDNA, we can see that SG showed high fluorescence intensity due to its high enhancement of fluorescence after interaction with DNA duplexes (Figure 2, line e). These results illustrate that, in the proposed strategy, the fluorescence signal only comes from the specific interaction between SG and the formed dsDNA, guaranteeing a good signal-to-noise ratio for miRNAs detection.

At the same time, molecular dynamics (MD) simulations of four systems including ssDNA−graphene (Supporting Information Figure S1), dsDNA−graphene (Supporting Information Figure S2), partial hairpin probe−graphene (Supporting Information Figure S3), and complete hairpin probe−graphene (Supporting Information Figure S4) were carried out for 30 ns using Assisted Model Building with Energy Refinement (AMBER) package to study the interaction of different types of DNA and graphene molecule in aqueous solution, respectively.[49] The molecular mechanics/Poisson−Boltzmann surface area (MM-PBSA) method is used to calculate the binding free energies from 100 snapshots which are extracted from MD trajectories.[50] The binding free energies of ssDNA−graphene, dsDNA−graphene, partial hairpin probe−graphene, and complete hairpin probe−graphene are −21.74, 33.76, −44.19, and 93.66 kcal/mol, respectively. The negative value of the binding free energies of ssDNA−graphene and partial hairpin probe−graphene means tight binding of ssDNA and partial hairpin probe to the GO. The lower energy of partial hairpin probe−GO than that of ssDNA−GO is mainly owed to van der Waals interactions which are affected by the distance between the molecules. In partial hairpin probe, the distance between the single-strand fragment and GO can be regulated

dx.doi.org/10.1021/ac500752t | Anal. Chem. 2014, 86, 5487−5493

Scheme 1. Illustration of the Graphene Fluorescence Switch-Based Cooperative Amplification for Target miRNAs

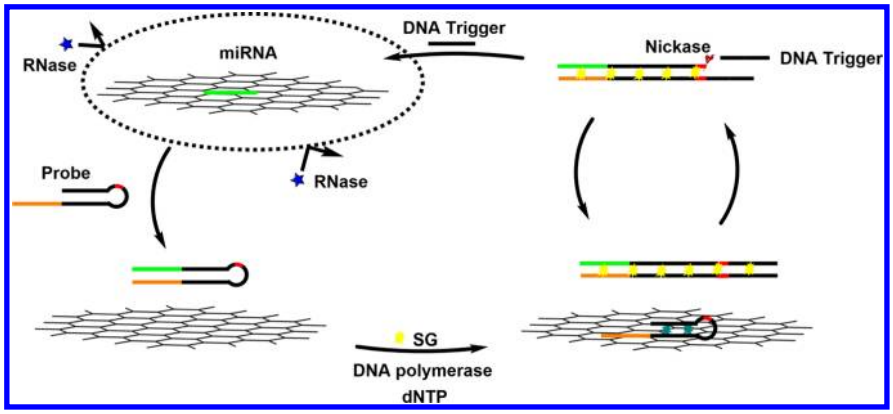

by its direct connected double-strand fragment. The increased distance between the single-strand fragment and GO can lead to a corresponding increased attraction and lower binding free energies. The positive value of the binding free energies of complete hairpin probe and dsDNA means these two types of DNA are free of the GO. In this case, the entropy is the major factor for the binding free energy. The complete hairpin probe has more complementary bases and bigger molecular weight than the dsDNA, leading to smaller value of the entropy and higher energy of complete hairpin probe−graphene than that of dsDNA−graphene. The conclusion is supported by Supporting Information Figures S1−S4 which plot the time evolution of the four systems. It is apparent from Supporting Information Figures S2 and S4 that the dsDNA and complete hairpin probe quickly unpack from the GO. However, as seen from Supporting Information Figures S1 and S3, the ssDNA and the single-strand segment of the partial hairpin probe remain well binding with graphene; the single-strand segment of the partial hairpin probe produces more contacts with the graphene than the ssDNA.

Principle of the Graphene Fluorescence Switch-Based Circular Exponential Amplification Assay for miRNAs. The proposed strategy of miRNAs detection is illustrated in Scheme 1. First, GO was added to the target miRNA solution. In the presence of GO, the target miRNA can bind strongly to the GO surface via $\pi-\pi$ stacking and be protected from enzymatic digestion effectively. Then, a designed partial hairpin probe containing an miRNA-binding domain (orange), a recognition domain for nicking enzyme (red), and an amplification domain (black) was introduced into the system and hybridized with the target miRNA to form the complete hairpin structure, inducing the desorption of miRNA from the GO surface. In the presence of Vent (exo-) DNA polymerase and dNTPs, the target miRNA extended along the template to unfold the hairpin probe and form a complete duplex. Subsequently, the nicking enzyme recognized the duplex site and cleaved the DNA strand, generating a new short DNA trigger with the same sequence as the miRNA. The released more stable DNA triggers were preferred as the primers to initiate a new extension reaction. Through the repeated extension, cleavage, and the release of short DNA, a new circular exponential amplification for the target miRNA was achieved. In order to obtain higher detection sensitivity, an intercalating dye SG was used in the assay. SG showed high selectivity and detection sensitivity toward the formed dsDNA detached from the GO surface due to its high enhancement of fluorescence upon interaction with DNA duplexes,[45] while fluorescence derived from the SG inserted into the stem of the partial hairpin probe was efficiently quenched by the GO as a result of the noncovalent adsorption. Compared with traditional DNA labeling with fluorescence dyes in a 1:1 stoichiometric ratio, the multimolecules binding of the SG to dsDNA can lead to stronger fluorescence signal and allow the method to have higher detection sensitivity. Due to the extraordinary fluorescence quenching of GO, an efficient signal-to-noise ratio enhancement for miRNAs detection also can be obtained by the SG/GO system.

The proposed detection system was confirmed by the measurement of fluorescent spectra and gel electrophoresis. As shown in Figure 3A, after the GO, DNA polymerase, dNTP, and SG were added, the detection system only containing hairpin probe (HP) or containing HP and nicking endonuclease showed faint fluorescence in the absence of target miRNA (Figure 3A, curves a and b). Small enhancement of fluorescence was observed when HP and miRNA were introduced into the detection system (Figure 3A, curve c), indicating that only hybridization and extension reaction occurred and a linear assay was achieved. In the system containing not only HP and miRNA but also nickase, a large number of DNA triggers were generated through the repeated extension, cleavage, and the release of short oligonucleotides. The circular exponential amplification assay for miRNA generated the highest fluorescence signal (Figure 3A, curve d). To verify the cleavage by nicking endonuclease, PAGE was also performed. After triggering by the let-7a, the reaction was conducted and productions were analyzed using 16% PAGE. Lane 1 in the inset of Figure 3 shows the amplification products in the presence of let-7a, HP, and nicking endonuclease. A 73-base-long product was observed because DNA polymerase extended the 3′ end of HP on the HP template and converted the HP to a 73-base-long product. Also, the about 60-base-long product is assumed to be corresponding to be the HP. Due to the cleavage of the endonuclease, the circular amplification products are far more than the unreacted HP. When the target miRNA reacted with HP in the absence of endonuclease, only a linear assay consisting of hybridization and extension reaction occurred; thus, few complete dsDNA products were produced and a lot of unreacted HP remained in the system (Figure 3 inset, lane 2). In the control experiment, no complete dsDNA product was observed because of no target miRNA added (Figure 3 inset, lane 3).

In most reported circular enzymatic amplification assay, the target miRNA was released and used as new trigger to initiate next reaction cycle.[33,34] The free miRNA from GO is

dx.doi.org/10.1021/ac500752t | Anal. Chem. 2014, 86, 5487−5493

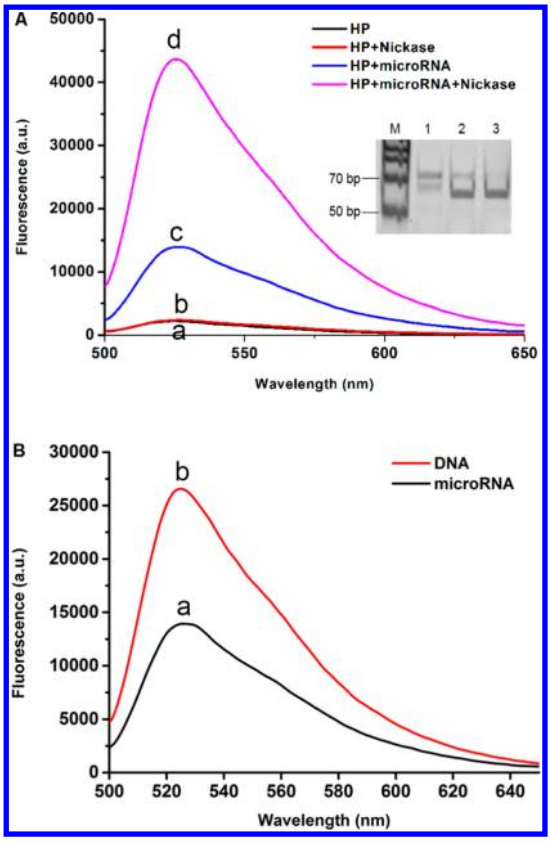

Figure 3. (A) Fluorescence intensity of the detection system containing HP (a), HP and endonuclease (b), HP and let-7a (c), and HP, miRNA, and endonuclease (d) in the presence of GO, SG, DNA polymerase, and dNTP. Inset: polyacrylamide gel electrophoresis (16%) of products of the detection system containing HP, nicking endonuclease, and let-7a (lane 1), HP and let-7a (lane 2), and only let-7a (lane 3) in the presence of GO, SG, DNA polymerase, and dNTP. The products were stained with SG. The marker is indicated by M. (B) Fluorescence intensity of the detection system using the same amount of miRNA (a) and DNA (b) triggers, respectively. The reaction solution contained 12 nM HP and 0.12 nM miRNA or 0.12 nM DNA.

susceptible to enzymatic degradation due to its special 2′-hydroxyl groups which act as nucleophiles.[51] So, in the proposed assay, a DNA fragment with the same sequences as the target miRNA was designed to be used as new triggers. The fluorescence intensity generated from the linear assay using DNA and miRNA as triggers was compared. Respectively, the same amount of DNA and the miRNA were added into the detection system containing GO, HP, DNA polymerase, and dNTP, initiating the hybridization and extension reaction. After staining with SG, fluorescence intensity of the products was detected. As shown in Figure 3B, the fluorescence signal generated by DNA triggers reached 26 560, which is 1.9-fold more than that generated by miRNA, suggesting the DNA triggers are preferred for the sustained reaction.

Kinetics of Reaction. The kinetic process of the circular exponential amplification was studied by monitoring the fluorescence change after the GO-protected miRNA was introduced into the detection system. Following the extension, cleavage and the repeated circular exponential amplification, an increase in fluorescence intensity was observed. As shown in Figure 4, at the beginning, slow increase in fluorescence intensity was observed because the concentration of target

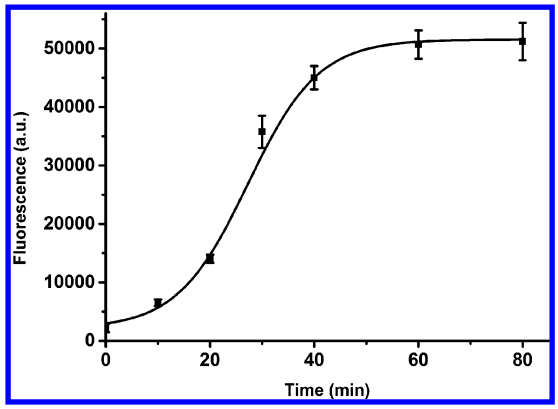

Figure 4. Kinetic response of the amplification reaction. The reaction solution contained 12 nM hairpin probe and 0.12 nM let-7a. The error bar represents the standard deviation of three measurements.

miRNA and released DNA triggers was low. Subsequently, an immediate rise in fluorescence intensity was observed, signifying the formation of circular exponential amplification after quick cleavage of the duplex and release of universal DNA triggers. After 50 min, the fluorescence intensity increased to a platform due to the depletion of the reaction components, such as dNTP or HP. These results further confirm that the designed circular exponential amplification occurred as expected and the detection of miRNAs can be accomplished within 2 h.

Specificity of the Assay. It is a great challenge to carry out the miRNAs assay with high specificity due to the high sequence homology among family members and small size of miRNAs. For example, members of the let-7 miRNA family differ by only one or two nucleotides in sequence with the same length (only 22 bases). The selectivity of the proposed strategy was investigated by miRNAs let-7a, let-7b, let-7c, and miR-21 with the same concentration. Using a hairpin probe containing a perfectly complementary domain to let-7a, fluorescence intensity produced by let-7a is 4.3-, 3.4-, and 5.9-fold of that produced by let-7b, let-7c, and miR-21, respectively (Figure 5). These results suggest that the proposed miRNAs detection approach has high sequence specificity to discriminate the

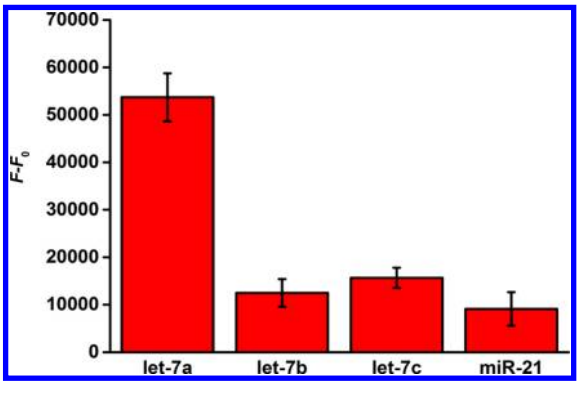

Figure 5. Comparison of the fluorescence intensity produced by let-7a, let-7b, let-7c, and miR-21 using a hairpin probe containing a complementary domain to let-7a, where F and F_0 are fluorescence intensities of amplification products by the reaction in the presence and absence of miRNAs, respectively. The reaction solution contained 12 nM hairpin probe and 0.12 nM let-7a, let-7b, let-7c, and miR-21. The error bar represents the standard deviation of three measurements.

dx.doi.org/10.1021/ac500752t | Anal. Chem. 2014, 86, 5487−5493

perfectly complementary target and the mismatched strands and has potential application in single-nucleotide polymorphism analysis.

Sensitivity of the Assay. Detection conditions such as the concentration of HP and the temperature of reaction were optimized to improve the detection sensitivity. The results are shown in Figure S5 (Supporting Information). Finally, 12 nM HP was selected and 55 °C was considered to be the optimal reaction temperature. Under the optimized conditions, the let-7a was detected to evaluate the sensitivity of the proposed strategy. Fluorescent intensities of products via the reaction with different amounts of let-7a were measured (Figure 6), and

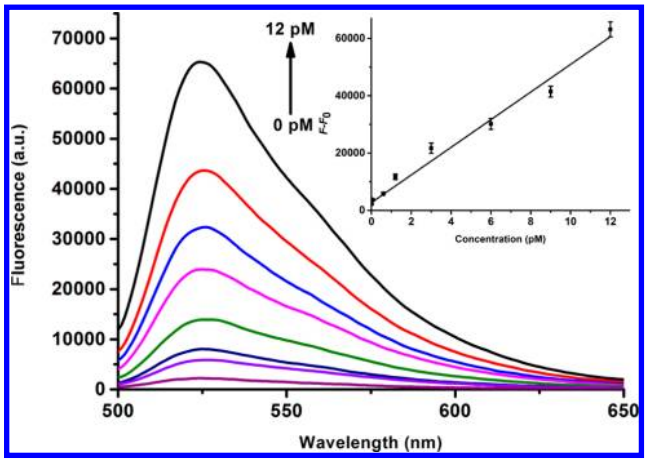

Figure 6. Relationship between the fluorescent response and the concentration of target miRNA (let-7a). The reactions were conducted with 12 nM hairpin probe and miRNA from 0.06 to 12 pM.

there was a remarkable increase with more amount of let-7a. A good linearity was obtained in 3 orders of magnitude from 0.06 to 12 pM miRNA. The correlation equation is $F - F_0 = 2715.37 + 4820.75C$ (F and F_0 represent fluorescence intensities of amplification products by the reaction in the presence and absence of let-7a; C represents the concentration of let-7a, pM) with a correlation coefficient $r = 0.9904$. A relative standard deviation (RSD) of 3.8% for 11 repetitive measurements of 6 pM let-7a was obtained, providing a good reproducibility of this miRNA assay. The detection limit is estimated to be 10.8 fM (3σ, $n = 11$). The low detection limit allows sensitive and accurate quantitation of miRNA at low concentrations, which is of great significance in the early diagnosis of diseases. A control experiment for target let-7a detection without GO was also conducted. The detection limit is calculated to be 14.7 nM. The lower detection sensitivity may caused by the high fluorescence background induced by SG binding to the hairpin probe and the digestion of partial target miRNA in the absence of GO.

Real Sample Assay. To demonstrate the capability of the proposed method in real sample analysis, we perform the miRNA assay using human lung cells. The concentration of let-7a in human lung cells was determined by the standard addition method using synthetic let-7a as the standard. Aliquots of the human lung total RNA (1.8 μg/μL, 1 μL) extracted from human lung cells were spiked with standard solutions containing synthetic let-7a at concentrations of 0.1, 0.2, 0.3, 0.4, 0.5, 0.6, and 0.7 pM, respectively. Then, the reaction and fluorescence detection were performed under the conditions as described in the Experimental Section. The results are shown in Supporting Information Figure S6. The content of let-7a in the human lung total RNA sample is calculated at 5.22×10^9 copies/μg, which is in good agreement with that obtained in previous studies.[30,52,53]

CONCLUSIONS

In summary, we have developed a sensitive and accurate assay for miRNAs on the basis of cooperative amplification combining with the GO fluorescence switch-based circular exponential amplification and the multimolecules labeling of SG. Through repeated hybridization, extension, and enzymatic cleavage, a small amount target miRNA can be converted to a large number of stable DNA triggers and a new circular exponential amplification for miRNA was achieved. Unlike the miRNA released and used as new triggers to initiate the next cycle in most reported reactions, in this assay, the released DNA triggers are more stable and preferred for the sustained reaction. Moreover, multimolecules binding of the intercalating dye SG to dsDNA induced significant enhancement of fluorescence signal and further improved the detection sensitivity. The GO can protect the target miRNA from enzymatic digestion effectively after the noncovalent adsorption of miRNA on its surface. As a fluorescence switch, the GO also can guarantee the high signal-to-noise ratio. This assay exhibited excellent specificity to discriminate single-nucleotide difference and allowed quantification of miRNA with a sensitivity of 10.8 fM. The miRNA analysis in human lung cells was also performed, indicating that this strategy will become a sensitive and reliable miRNAs quantification method in biomedical research and early clinical diagnostics.

ASSOCIATED CONTENT

Supporting Information

Process of molecular dynamics simulation, calculations of binding free energies, and Figures S1–S6. This material is available free of charge via the Internet at http://pubs.acs.org.

AUTHOR INFORMATION

Corresponding Author

*E-mail: tangb@sdnu.edu.cn. Phone: 86 531 86180010. Fax: 86 531 86180017.

Author Contributions

†H.L. and L.L. contributed equally to this work.

Notes

The authors declare no competing financial interest.

ACKNOWLEDGMENTS

This work was supported by the 973 Program (2013CB933800), the National Natural Science Foundation of China (21227005, 21390411, 91313302, 21035003, 21205074, 31200545), and the Program for Changjiang Scholars and Innovative Research Team in University.

REFERENCES

(1) Ventura, A.; Jacks, T. *Cell* **2009**, *136*, 586.
(2) Rossi, J. J. *Cell* **2009**, *137*, 990.
(3) Johnson, S. M.; Grosshans, H.; Shingara, J.; Byrom, M.; Jarvis, R.; Cheng, A.; Labourier, E.; Reinert, K. L.; Brown, D.; Slack, F. J. *Cell* **2005**, *120*, 635.
(4) He, L.; Thomson, J. M.; Hemann, M. T.; Hernando-Monge, E.; Mu, D.; Goodson, S.; Powers, S.; Cordon-Cardo, C.; Lowe, S. W.; Hannon, G. J.; Hammond, S. M. *Nature* **2005**, *435*, 828.
(5) Calin, G. A.; Croce, C. M. *Nat. Rev. Cancer* **2006**, *6*, 857.

(6) Sawyers, C. L. *Nature* **2008**, *452*, 548.
(7) Tricoli, J. V.; Jacobson, J. W. *Cancer Res.* **2007**, *67*, 4553.
(8) Ryan, B. M.; Robles, A. I.; Harris, C. C. *Nat. Rev. Cancer* **2010**, *10*, 389.
(9) Mitchell, P. S.; Parkin, R. K.; Kroh, E. M.; Fritz, B. R.; Wyman, S. K.; Pogosova-Agadjanyan, E. L.; Peterson, A.; Noteboom, J.; O'Briant, K. C.; Allen, A.; Lin, D. W.; Urban, N.; Drescher, C. W.; Knudsen, B. S.; Stirewalt, D. L.; Gentleman, R.; Vessella, R. L.; Nelson, P. S.; Martin, D. B.; Tewari, M. *Proc. Natl. Acad. Sci. U.S.A.* **2008**, *105*, 10513.
(10) Cao, Y.; DePinho, R. A.; Ernst, M.; Vousden, K. *Nat. Rev. Cancer* **2011**, *11*, 749.
(11) Chen, C.; Ridzon, D. A.; Broomer, A. J.; Zhou, Z.; Lee, D. H.; Nguyen, J. T.; Barbisin, M.; Xu, N. L.; Mahuvakar, V. R.; Andersen, M. R.; Lao, K. Q.; Livak, K. J.; Guegler, K. J. *Nucleic Acids Res.* **2005**, *33*, e179.
(12) Valoczi, A.; Hornyik, C.; Varga, N.; Burgyan, J.; Kauppinen, S.; Havelda, Z. *Nucleic Acids Res.* **2004**, *32*, e175.
(13) Varallyay, E.; Burgyan, J.; Havelda, Z. *Methods* **2007**, *43*, 140.
(14) Babak, T.; Zhang, W.; Morris, Q.; Blencowe, B. J.; Hughes, T. R. *RNA* **2004**, *10*, 1813.
(15) Nelson, P. T.; Baldwin, D. A.; Scearce, L. M.; Oberholtzer, J. C.; Tobias, J. W.; Mourelatos, Z. *Nat. Methods* **2004**, *1*, 155.
(16) Thomson, J. M.; Parker, J.; Perou, C. M.; Hammond, S. M. *Nat. Methods* **2004**, *1*, 47.
(17) Liang, R. Q.; Li, W.; Li, Y.; Tan, C. Y.; Li, J. X.; Jin, Y. X.; Ruan, K. C. *Nucleic Acids Res.* **2005**, *33*, e17.
(18) Beuvink, I.; Kolb, F. A.; Budach, W.; Garnier, A.; Lange, J.; Natt, F.; Dengler, U.; Hall, J.; Filipowicz, W.; Weiler, J. *Nucleic Acids Res.* **2007**, *35*, e52.
(19) Lee, J. M.; Jung, Y. *Angew. Chem., Int. Ed.* **2011**, *50*, 12487.
(20) Tu, Y. Q.; Wu, P.; Zhang, H.; Cai, C. X. *Chem. Commun.* **2012**, *48*, 10718.
(21) Xu, F.; Dong, C.; Xie, C.; Ren, J. *Chem.—Eur. J.* **2010**, *16*, 1010.
(22) Wang, Y.; Zheng, D.; Tan, Q.; Wang, M. X.; Gu, L. Q. *Nat. Nanotechnol.* **2011**, *6*, 668.
(23) Dong, H.; Lei, J.; Ju, H.; Zhi, F.; Wang, H.; Guo, W.; Zhu, Z.; Yan, F. *Angew. Chem., Int. Ed.* **2012**, *51*, 4607.
(24) Degliangeli, F.; Kshirsagar, P.; Brunetti, V.; Pompa, P. P.; Fiammengo, R. *J. Am. Chem. Soc.* **2014**, *136*, 2264.
(25) Cissell, K. A.; Rahimi, Y.; Shrestha, S.; Hunt, E. A.; Deo, S. K. *Anal. Chem.* **2008**, *80*, 2319.
(26) Allawi, H. T.; Dahlberg, J. E.; Olson, S.; Lund, E.; Olson, M.; Ma, W. P.; Takova, T.; Neri, B. P.; Lyamichev, V. I. *RNA* **2004**, *10*, 1153.
(27) Hartig, J. S.; Grune, I.; Najafi-Shoushtari, S. H.; Famulok, M. *J. Am. Chem. Soc.* **2004**, *126*, 722.
(28) Hackenberg, M.; Sturm, M.; Langenberger, D.; Falcon-Perez, J. M.; Aransay, A. M. *Nucleic Acids Res.* **2009**, *37*, W68.
(29) Jia, H.; Li, Z.; Liu, C.; Cheng, Y. *Angew. Chem., Int. Ed.* **2010**, *49*, 5498.
(30) Liu, H.; Li, L.; Duan, L.; Wang, X.; Xie, Y.; Tong, L.; Wang, Q.; Tang, B. *Anal. Chem.* **2013**, *85*, 7941.
(31) Bi, S.; Zhang, J.; Hao, S.; Ding, C.; Zhang, S. *Anal. Chem.* **2011**, *83*, 3696.
(32) Wang, G. L.; Zhang, C. Y. *Anal. Chem.* **2012**, *84*, 7037.
(33) Zhu, X.; Zhou, X.; Xing, D. *Chem.—Eur. J.* **2013**, *19*, 5487.
(34) Cui, L.; Lin, X. Y.; Lin, N. H.; Song, Y. L.; Zhu, Z.; Chen, X.; Yang, C. J. *Chem. Commun.* **2012**, *48*, 194.
(35) Novoselov, K. S.; Geim, A. K.; Morozov, S. V.; Jiang, D.; Zhang, Y.; Dubonos, S. V.; Grigorieva, I. V.; Firsov, A. A. *Science* **2004**, *306*, 666.
(36) Li, D.; Kaner, R. B. *Science* **2008**, *320*, 1170.
(37) Tang, L.; Chang, H.; Liu, Y.; Li, J. *Adv. Funct. Mater.* **2012**, *22*, 3083.
(38) Swathi, R. S.; Sebastian, K. L. *J. Chem. Phys.* **2009**, *130*, 086101.
(39) Swathi, R. S.; Sebastian, K. L. *J. Chem. Phys.* **2008**, *129*, 054703.
(40) Cui, L.; Chen, Z.; Zhu, Z.; Lin, X.; Chen, X.; Yang, C. J. *Anal. Chem.* **2013**, *85*, 2269.
(41) Tang, Z.; Wu, H.; Cort, J. R.; Buchko, G. W.; Zhang, Y.; Shao, Y.; Aksay, I. A.; Liu, J.; Lin, Y. *Small* **2010**, *6*, 1205.
(42) Dong, H.; Zhang, J.; Ju, H.; Lu, H.; Wang, S.; Jin, S.; Hao, K.; Du, H.; Zhang, X. *Anal. Chem.* **2012**, *84*, 4587.
(43) Tu, Y.; Li, W.; Wu, P.; Zhang, H.; Cai, C. *Anal. Chem.* **2013**, *85*, 2536.
(44) Hu, X.; Mu, L.; Wen, J.; Zhou, Q. *J. Hazard. Mater.* **2012**, *213-214*, 387.
(45) Zipper, H.; Brunner, H.; Bernhagen, J.; Vitzthum, F. *Nucleic Acids Res.* **2004**, *32*, e103.
(46) He, S.; Song, B.; Li, D.; Zhu, C.; Qi, W.; Wen, Y.; Wang, L.; Song, S.; Fang, H.; Fan, C. *Adv. Funct. Mater.* **2010**, *20*, 453.
(47) Wang, Y.; Li, Z.; Wang, J.; Li, J.; Lin, Y. *Trends Biotechnol.* **2011**, *29*, 205.
(48) Wang, Y.; Chang, H.; Wu, H.; Liu, H. *J. Mater. Chem.* **2013**, *1*, 3521.
(49) Kumar, S.; Rosenberg, J. M.; Bouzida, D.; Swendsen, R. H.; Kollman, P. A. *J. Comput. Chem.* **1992**, *13*, 1011.
(50) Srinivasan, J.; Cheatham, T. E.; Cieplak, P.; Kollman, P. A.; Case, D. A. *J. Am. Chem. Soc.* **1998**, *120*, 9401.
(51) Li, Y.; Breaker, R. R. *J. Am. Chem. Soc.* **1999**, *121*, 5364.
(52) Cheng, Y.; Zhang, X.; Li, Z.; Jiao, X.; Wang, Y.; Zhang, Y. *Angew. Chem., Int. Ed.* **2009**, *48*, 3268.
(53) Bi, S.; Cui, Y.; Li, L. *Anal. Chim. Acta* **2013**, *760*, 69.